



Revolutionizing Dye Removal: Unleashing the Power of Liquid–Liquid Extraction Batch Process

Kedar Sahoo¹ · Uma Sankar Behera² · Sourav Poddar³ · Hun-Soo Byun²

Received: 1 May 2024 / Revised: 28 May 2024 / Accepted: 3 June 2024 / Published online: 11 June 2024
© The Author(s), under exclusive licence to Korean Institute of Chemical Engineers, Seoul, Korea 2024

Abstract

This study focuses on numerically optimizing key process parameters related to the liquid–liquid extraction batch process (LLEBP) technique for carrying out batch runs to remove methyl red effectively (MR) from dye effluent. LLEBP, a suitable industrial process for treating dye effluents, depends on the number of reaction parameters such as feed concentration, extraction time, and dye ratio (solution/solvent). The current research utilized a central composite design (CCD) of experiments along with numerical optimization techniques to optimize process parameters over a range of dye concentrations: (20–100) ppm, extraction time range 10–30 min, and dye ratio 1–3 mL/mL (solution/solvent). The batch runs performed at room temperature and a constant pH of 3, according to the experimental design criteria, suggest that maximum dye removal efficiency and distribution coefficient value could be achieved within the feed concentration range of (20–30) ppm, 20–30 min of extraction time, and 1–3 mL/mL of dye ratio (solution/solvent). Solvent capacity increases significantly within the (60–100) ppm feed concentration range. Numerical optimization with desirability function criteria identified optimal conditions: 20 ppm dye concentration, 30 min extraction time, and 3 mL/mL dye ratio ensuring maximum LLEBP yield. The current investigation achieved a 4% higher dye removal (%) of 85.682 compared to the previous study. The distribution coefficient and solvent capacity attained were 5.287 and 4.504 mg/L, respectively. The research enhances understanding of the optimization process for LLEBP in MR dye removal from textile effluent, surpassing previous findings within the same input range. The manuscript aims to maximize process optimization using CCD, promoting sustainable industry progress in line with UN sustainable development goals.

Keywords Central composite design · Distribution coefficient · Liquid–liquid extraction · Methyl red · Numerical optimization · Solvent capacity

Kedar Sahoo and Uma Sankar Behera have equally contributed and are first and second authors.

✉ Sourav Poddar
souravpoddarsxc@gmail.com

✉ Hun-Soo Byun
hsbyun@jnu.ac.kr

¹ Department of Chemical Engineering, National Institute of Technology, Warangal, Telangana 506004, India

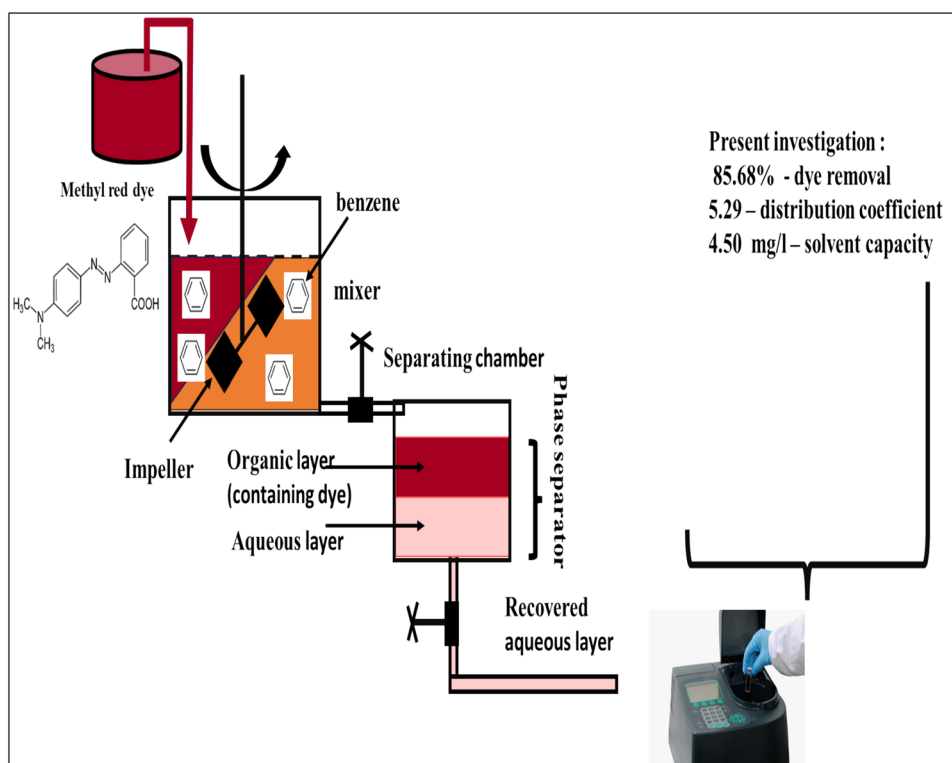
² Department of Chemical and Biomolecular Engineering, Chonnam National University, Yeosu, Jeonnam 59626, South Korea

³ Department of Chemical Engineering, Haldia Institute of Technology, Haldia, West Bengal 721657, India

Introduction

Natural water resources are currently under enormous stress, as their pollution problem has escalated to alarming levels. Synthetic dyes that are toxic and recalcitrant chemical substances present in wastewater pose a potential threat to natural water resources upon their ineffective discharge into them. The diversified application as a colouring agent in manufacturing textiles, polymer, pulp and paper, leather, and paint has created huge volumes (~280,000 tons annually) of waste dye solution [1, 2]. Coloured discharged effluent (even at < 1 mg/L), upon exposure to nearby water bodies, forms a film over the surface and obstructs sunlight penetration into it [3]. Therefore, it causes a reduction in the availability of sunlight intensity requisite for the photosynthesis of aquatic plants and dissolved oxygen levels. Since dyes in water are resistant to natural biodegradation,

Fig. 1 Schematic illustration of the process flow



an escalation in the total oxygen (O_2) needed to support both the chemical oxidation demand (COD) and biological oxidation demand (BOD) processes, ultimately causing water pollution [4–6]. Among manufacturing sectors, the textile industry is one of the most critical ones, and it is responsible for the generation of significant amounts of coloured wastewater as a byproduct of various textile manufacturing processes such as dyeing, finishing, and washing [7]. The coloured wastewater emanating from the textile industry is very complex (mixture of dye, pigment, heavy metal, and chemical) and needs to be treated cost-effectively, thus discharged to nearby water bodies. Nevertheless, the dyes' inherent toxicity and alarming side effects have created significant inquisitiveness among the scientific community to develop adequate "coloured wastewater" treatment strategies from environmental sustainability and ecosystem protection perspectives [8].

Among different dyes, anionic azo dyes account for ~60% of total dye usage in the textile industries [8]. From the manufacturing scenario, half of the 8 lakh tonnes annually produced dyes are azo dyes due to their high demand. Azo dyes are resistant to traditional treatment strategies, ultimately causing enhancement of total organic carbon and turbidity of exposed water bodies and acceleration of eutrophic processes. Besides, azo dyes are a reason for potential human

health hazards such as invoking allergies in the skin/eye/digestive tract, causing cell mutations and cancer on a long-term basis. Therefore, the efficacious removal of azo dyes from industrial effluents is desirable before they pollute nearby water bodies.

One such dye is methyl red (MR), an anionic mono-azo dye with ($-N=N-$) linkage. It is commonly encountered across printing and dyeing industries due to its high colour-fixing performance and less fading ability. As discussed earlier for azo dyes, if MR dye is ingested, it can induce irritation in the digestive tract, pharynx, eye, skin, etc. [9]. Additionally, MR can be converted into 2-aminobenzoic acid and mutagenic *N*-*N*-dimethyl-*p*-phenylene diamine. Techniques implemented earlier for the removal of MR dye from textile effluent are coagulation/flocculation [10], Fenton process [11, 12], peroxide oxidation [13], anaerobic digestion [14], bacterial degradation [15, 16] and adsorption [17], photocatalysis [18], etc. Though physical methods are non-destructive, they only encompass the inter-medium transfer of pollutants and thus require secondary treatment [19]. Similarly, the discussed chemical methods are not viable due to cost, low efficiency, high chemical dosage, and toxic byproduct generation problems [20–22]. Moderately oxidizing and thermal conditions and lengthy biological process time are also incapable of providing a viable solution [23].

Over the years, the adsorption method has been prevalent due to its low cost and efficacy, but sludge generation and separation are issues that cannot be circumvented [24].

Contrary to the above-stated physicochemical techniques, the LLEBP-mediated MR dye removal technique has recently gotten much attention. It is based on the mass transfer rate of solute distribution in a particular ratio between two immiscible solvents. LLEBP can achieve high throughput and purification under automated operation and has scale-up potential [25]. The solvents used in LLEBP are typically aqueous/organic, and solute is always transferred from the aqueous to the organic phase. The solute transfer process always proceeds through chemical energy interaction, and the chemical constituents of the solvents, apart from solute, always maintain a stable, low-free energy structure. Hence, the chemical compositions of used solvents remain unchanged during the solute exchange; ideally, the LLEBP process is well suited for low-volatility and heat-sensitive substances [26]. Various reports suggested the efficacy of using LLEBP to extract MR-like azo dyes. Pandit et al. [27] studied the successful elimination of anionic and cationic azo dyes from the liquid medium by encapsulating them in

reverse surfactant micelles in the solvent. Separating anionic dye (i.e. methyl orange) from the water was accomplished by forming reverse micelles of cationic surfactants (i.e. HTAB: hexadecyltrimethylammonium bromide surfactant) in amyl alcohol. The exact process was repeated for methylene blue (cationic) dye with the help of reverse micelles formed out of anionic surfactant (i.e. SDBS: sodium dodecyl benzene sulphonate) in an amyl alcohol solvent. Without surfactant use, only a small amount of dye extraction could have been possible by organic solvent.

Another azo dye, "1-diazo-2-naphthol-4-sulfonic acid", was successfully extracted from wastewater by using a solvent (trialkyl amine N_{235}), as reported by Hu et al. [28]. After extraction, the COD of raffinate was further controlled by catalytic oxidation of hydrogen peroxide to make it to national emission standard levels. LLEBP results showed that a single-stage extraction was responsible for ~82% of dye removal that can be enriched further to 93% under multistage operations.

Similarly, Yilmaz et al. [29] reported that LLEBP mediated removal of azo dyes from aqueous solutions using Calix (4) arene, b-cyclodextrin, and dichloromethane as

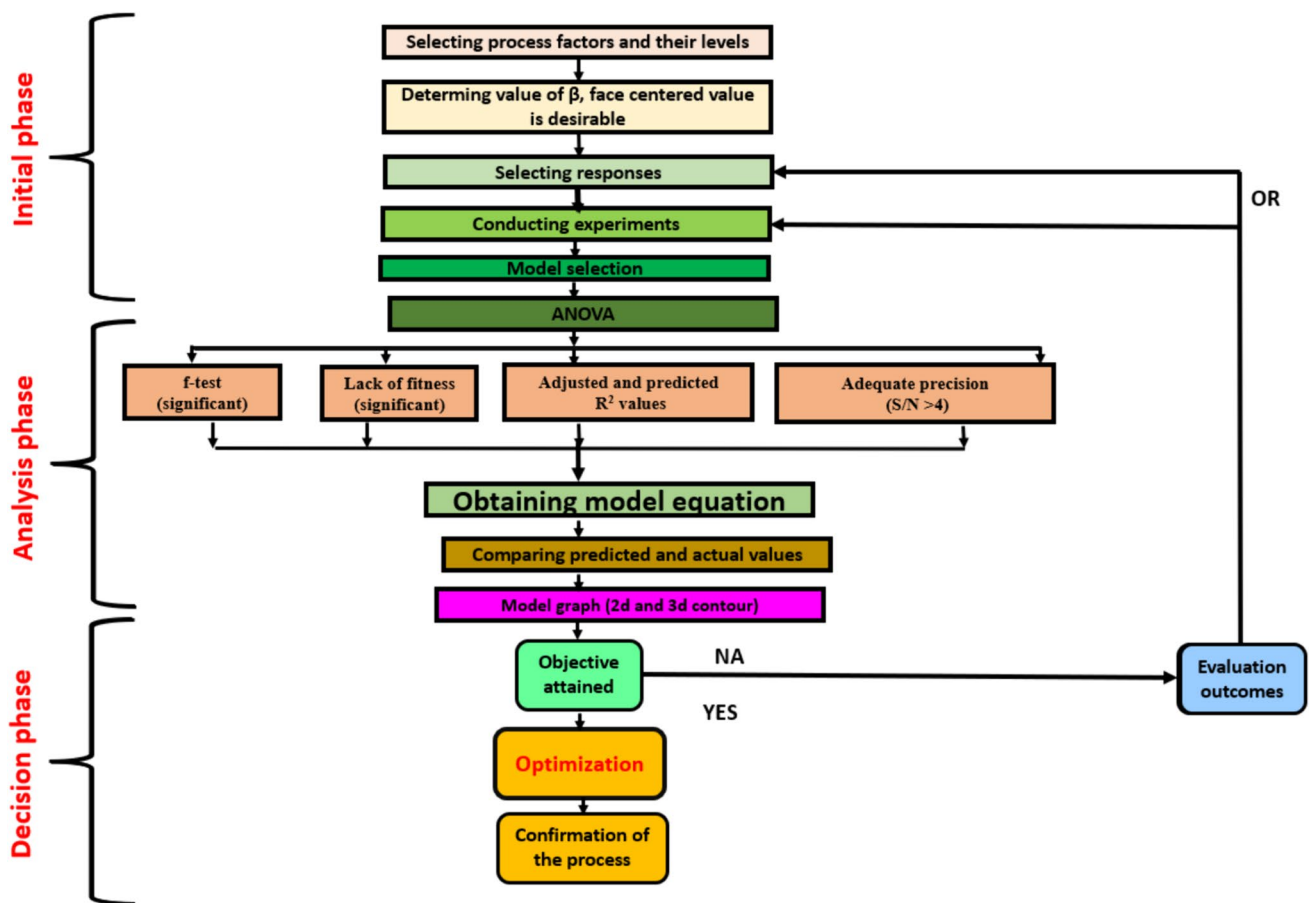


Fig. 2 Schematic flow diagram for CCD

Table 1 Independent parameters and levels considered for LLEBP of MR dye using benzene

Parameter	Designation	Unit of the quantity	Minimum	Maximum	Coded low	Coded high
Dye conc. in liquid	A	ppm	20.00	100.00	- 1 ↔ 20.00	+ 1 ↔ 100.00
Dye ratio (solution/solvent)	C	mL/mL	1.00	3.00	- 1 ↔ 1.00	+ 1 ↔ 3.00
Time of extraction	B	min	10.00	30.00	- 1 ↔ 10.00	+ 1 ↔ 30.00

extractants. LLEBP using propylene and 1,2-butylenes carbonates showed superior results compared to the conventional cloud point technique. While the cloud point technique resulted in recoveries ranging from 10 to 49%, the LLEBP process achieved nearly complete recovery at around 100% [30].

Another LLEBP process was investigated by Muthuraman et al. [31] to extract methylene blue from industrial wastewater. Benzoic acid was used as an extractant. Optimized process conditions suggested that ~99% of the dye was extracted from the aqueous phase, and the dye was recovered with the help of sulphuric acid solutions. The same research group also reported the LLEBP extraction study of anionic azo dye compound "golden yellow low salt" from water using tri-*n*-butyl phosphate as the carrier solvent. The extracted dye was stripped again using sodium hydroxide solutions [32].

Another azo dye removal technique was reported by Abbasi et al. [33], designed for methylene blue removal from polluted water by employing a mono- and di-ester mixture (MDEHPA) as the extractant within a Y–Y junction micro-channel. The investigation involved the optimization of process parameters such as pH, concentration of extractant, and residence time. The study reported a maximum extraction capacity of 98.4%, highlighting the benefit of MDEHPA in dye removal. There are few studies regarding LLEBP extraction of MR dye from wastewater; one of the reports was published by Muthuraman et al. [25]. They investigated an LLEBP system where MR dye was separated from an aqueous solution using a solvent like xylene as an extractant. The dye removal efficiency increased with extraction time, and the distribution ratio value was also reasonably high. After extraction, the dye was stripped out of the organic phase using sodium hydroxide solvent, and the reported results were on par with industrial standards.

Since several parameters need to be optimized in liquid–liquid extraction to obtain a suitable process yield [28], Kanakasabai et al. [34] discussed the process optimization aspects. Their study adopted a response surface methodology (RSM) with Box–Behnken design (BBD) mathematical technique to optimize the batch parameters of LLEBP for MR dye removal. The current study is a modification of their reported work where more accurate and best batch optimization data were obtained by incorporating a robust

CCD of the experiment method. The optimization results of the current study suggest the superiority of CCD in optimizing LLEBP for dye removal, and the augmented value of % dye removal, distribution coefficient, and solvent capacity could be achieved. This article carefully illustrates the comprehensive details of the LLEBP optimization technique and subsequent implications of the design data in the batch study to obtain suitable MR dye removal efficacy. This study also demonstrates that the extraction process can be fine-tuned to push its boundary limit by maintaining the same old experimental input range. The manuscript primarily focuses on maximizing process optimization using RSM CCD techniques. In this connection, Design-Expert version 13 was employed. Its statistical rigour ensures reliable results while minimizing experimental costs and resource consumption. Compared to traditional methods, CCD-RSM offers robust and reproducible optimization outcomes. Currently, the advancement of the research is in the progress of a sustainable industry which aligns with UN (United Nations) sustainable development goals such as clean water and sanitation (Goal 6), decent work and economic growth (Goal 8), and industry innovation and infrastructure (Goal 9). Our research aims to contribute significantly to addressing critical global challenges and promoting sustainable development.

Experimental Procedure

This section provides comprehensive information about the chemicals used for the batch reaction and outlines the standard experimental procedure followed.

Materials

The methyl red (MR) dye was purchased from nearby local vendors and used directly. Benzene purchased from SRL Pvt. Ltd. (99.7% assay) acted as a solvent in this study. Double-distilled (DD) water was procured from a local vendor with a pH of 5.96. HCl (35–38%), NaCl (> 99%), and NaOH (> 98%) were bought from SD Fine Chemicals Ltd., Merck Pvt. Ltd. and SRL Pvt. Ltd., respectively. Starch, Na₂CO₃, and NaHCO₃ were procured from Alfa Aesar, USA. All the chemicals were directly utilized in the experiment without additional purification.

Table 2 Predicted responses from the CCD technique for optimizing LLEBP process parameters and comparison with actual batch run results

Run	Factor 1 A: Dye concentration	Factor 2 B: Time of extraction	Factor 3 C: Dye ratio (solution/solvent)	Response 1 (predicted) Y1 (removal of dye)	Response 1 (actual) Y1	Response 2 (predicted) Y2 (coefficient of distribution)	Response 2 (actual) Y2	Response 3 (predicted) Y3 (solvent capacity)	Response 3 (actual) Y3
Unit	ppm	min	mL/mL	%	%	–	–	mg/L	mg/L
1	20	20	1	69.42	69.45	4.28	4.30	13.88	13.90
2	60	20	2	68.57	68.60	4.23	4.20	20.57	20.60
3	60	10	3	58.28	58.25	3.59	4.00	11.65	11.70
4	60	20	2	67.71	67.70	4.17	4.20	20.31	20.30
5	60	20	2	66.85	66.86	4.12	4.10	20.05	20.00
6	20	20	3	81.42	81.45	5.02	5.00	5.42	5.40
7	60	10	1	45.42	45.45	2.8	2.80	27.25	27.30
8	20	10	2	46.28	46.30	2.85	2.80	4.62	4.60
9	100	30	2	57.42	57.40	3.54	3.50	28.71	28.70
10	100	20	1	47.14	47.15	2.9	2.90	47.14	47.10
11	20	30	2	80.57	80.60	4.97	5.00	8.05	8.06
12	60	30	1	56.57	56.55	3.49	3.50	33.94	34.00
13	100	20	3	55.71	55.70	3.43	3.40	18.57	18.60
14	60	30	3	66	66.04	4.07	4.00	13.2	13.05
15	100	10	2	48	47.98	2.96	3.00	24	23.85
16	60	20	2	66.85	66.90	4.12	4.10	20.05	20.00
17	20	20	3	81.42	81.40	5.02	5.00	5.42	5.40
18	60	10	1	45.42	45.45	2.8	2.80	27.25	27.30
19	20	10	2	46.28	46.30	2.85	2.90	4.62	4.60
20	60	30	1	56.57	56.60	3.49	3.50	33.94	34.00

Preparation of Model Textile Effluent Containing MR Dye

An additive package containing a sizing and fixing agent, a neutralizing agent, a hydrolyzing agent, and a pH-controlling agent was mixed with the model dye solution to create an environment similar to the textile effluent[23]. Starch acted as a sizing agent, Na_2CO_3 , NaHCO_3 , and NaCl as fixing agents, and NaOH as a hydrolyzing agent; the pH was controlled by adding HCl .

LLEBP Experimentation

Before batch LLEBP experiments, MR dye concentrations were calibrated in the concentration range (20–100) ppm by considering its absorbance maxima, i.e. $\lambda_{\text{max}} = 491$ nm, [within the wavelength range of (370–600) nm, and temperature of (298 ± 0.2) K] in a UV–Vis spectrophotometer (Cary 60 UV–Vis, Agilent, USA). The interference of other dye effluent components was also considered during calibration. Generally, starch concentration was the primary factor to be considered; hence, it was subtracted from calibrated data,

but other additives did not show significant absorbance at the spectral wavelength.

Figure 1 shows the detailed LLEBP process diagram. According to the design data, the initial dye concentration in the feed solution was chosen and vigorously blended with the benzene solvent. The system reached equilibrium, and phase separation was achieved in a separating funnel. Two distinct layers, characterized as the extract (upper layer) and the raffinate (lower layer) phase, were identified in the separating funnel. The remaining dye concentration in the raffinate phase was calculated using UV–visible spectrophotometer and calibration data.

Industrial processes like LLEBP are complex techniques involving several process parameters that need to be optimized, such as solute concentration, solute–solvent ratio, reaction time, etc., to obtain the desired output response. The desired process output responses studied/improved in the current manuscript are dye removal percentage, solvent capacity, and distribution coefficient. These are defined in Eqs. (1–3).

Table 3 ANOVA of % dye removal response using the quadratic model

Source	% Dye removal				Distribution coefficient				Solvent capacity						
	S*	Dof*	M*	F*	P*	SS	Dof*	MS	F-magnitude	P-magnitude	SS	Dof*	MS	F-magnitude	P-magnitude
Model	2634.29	9	292.70	13.72	0.0002	10.04	9	1.12	13.64	0.0002	2506.46	9	278.50	446.73	<0.0001
A—dye concentration (in feed)	655.73	1	655.73	30.73	0.0002	2.51	1	2.51	30.65	0.0002	1080.65	1	1080.65	1733.44	<0.0001
B—extraction time	608.57	1	608.57	28.52	0.0003	2.33	1	2.33	28.49	0.0003	39.60	1	39.60	63.53	<0.0001
C—dye solution/ solvent (ratio)	313.24	1	313.24	14.68	0.0033	1.19	1	1.19	14.55	0.0034	845.69	1	845.69	1356.54	<0.0001
AB	245.67	1	245.67	11.51	0.0069	0.9418	1	0.9418	11.52	0.0068	0.9347	1	0.9347	1.50	0.2488
AC	8.85	1	8.85	0.4148	0.5341	0.0336	1	0.0336	0.4117	0.5356	111.84	1	111.84	179.40	<0.0001
BC	0.1754	1	0.1754	0.0082	0.9296	0.0007	1	0.0007	0.0087	0.9276	9.60	1	9.60	15.40	0.0028
A ²	11.01	1	11.01	0.5161	0.4890	0.0425	1	0.0425	0.5205	0.4872	19.55	1	19.55	31.36	0.0002
B ²	368.61	1	368.61	17.27	0.0020	1.39	1	1.39	17.03	0.0021	13.59	1	13.59	21.81	0.0009
C ²	19.20	1	19.20	0.8996	0.3653	0.0733	1	0.0733	0.8971	0.3659	40.97	1	40.97	65.72	<0.0001
Residual	213.41	10	21.34			0.8173	10	0.0817			6.23	10	0.6234		
Lack of fit	211.38	3	70.46	242.50	<0.0001	0.8091	3	0.2697	230.23	<0.0001	6.05	3	2.02	75.91	<0.0001
Pure error	2.03	7	0.2906			0.0082	7	0.0012			0.1859	7	0.0266		
R ²	0.9251					0.9247					0.9975				
Cor total	2847.71	19				10.85	19				2512.70	19			

S* sum of squares; M* mean square; Dof* degree of freedom; F* F-magnitude; P* P-magnitude; A: the concentration dye in the feed; B: extraction time; C: dye ratio (solution/solvent)

$$\% \text{Removal of dye} = \frac{a}{b} \times 100, \tag{1}$$

$$\text{Coefficient of distibution} = \frac{a}{b}, \tag{2}$$

$$\text{Solvent capacity (mg/l)} = (c/d) \times e, \tag{3}$$

where, *a* is the dye concentration in the extract; *b* is the dye concentration in the feed; *c* is the concentration of the dye extract; *d* is the volume of the solvent; *e* is the volume of the dye and also dye concentration in the extract = dye concentration in the feed – dye concentration in the raffinate.

LLEBP Parameters Optimization Using Design of Experiment (DOE)

Phase one: developing the core composite and response layers. As a dependable statistical method for applications in chemical processes, randomized controlled trials (RCTs) use various mathematical and statistical techniques to determine the optimal fit between empirical models and experimental data [35, 36]. The researchers employed RSM techniques for optimization and have extensively investigated CCD (central composite design), a method for fitting second-order polynomial equations, to simplify several research problems [37–39]. A CCD generally has three groups of design parameters in general [40, 41], which are as follows:

- A. The design points (2 *k*) of a two-level factorial or fractional factorial can have any combination of + 1 and – 1 levels of factors.
- B. 2 *k* axial points, also known as star points, are placed at a distance of α from the centre to produce quadratic terms; core values that stand for replicate words;
- C. core values give a solid and impartial assessment of the experimental inaccuracy.

Therefore, considering the above-said parameters, the number of experiments designed by CCD can be expressed as

$$P = k^2 + 2k + n. \tag{4}$$

The variables *P*, *k*, and *n* denote the total number of experiments, factors analysed, and replicates, respectively. The two most common tools used for central composite design under RSM are Minitab and Design Expert software. Software for optimization is utilized in this investigation using version number 13 of Design Expert developed by Stat-Ease. Figure 2 depicts the procedures that will be followed for the CCD. The computation of the alpha value is crucial in CCD because it can establish the position of the

axial points in the experimental region. The design can be spherical, orthogonal, rotatable, or face centred, depending on the beta (β) value. It is computed as a practical compromise between face centred and spherical:

$$\beta = [2^m]^{0.25}. \tag{5}$$

A desired beta value is 1, which guarantees the axial point is located within the factorial part region. It provides three tiers for the experimental design matrix, called face-focused design. A statistical analysis system's response surface regression process is used to analyse the experimental data. The results of fitting the independent variables and answers to a second-order polynomial equation yield the correlation between the two [7, 42–47].

$$T = \chi_o + \sum_{i=1}^k \chi_i y_i + \sum_{i=1}^k \chi_{ii} y_{ii}^2 + \sum_{i=1}^k \sum_{j=1}^k \chi_{ij} y_i y_j + \xi. \tag{6}$$

Here, T represents the responses, *k* is the total number of independent factors, χ_0 is an intercept, *i*, *ii*, and *ij* with χ represent the coefficient values for linear, quadratic, and interaction effects, respectively, and *xi* and *xj* in the above equation show the coded levels for independent variables [7, 48, 49]. The detailed process parameters are shown in Table 1.

Optimization Employing the Desirability Function

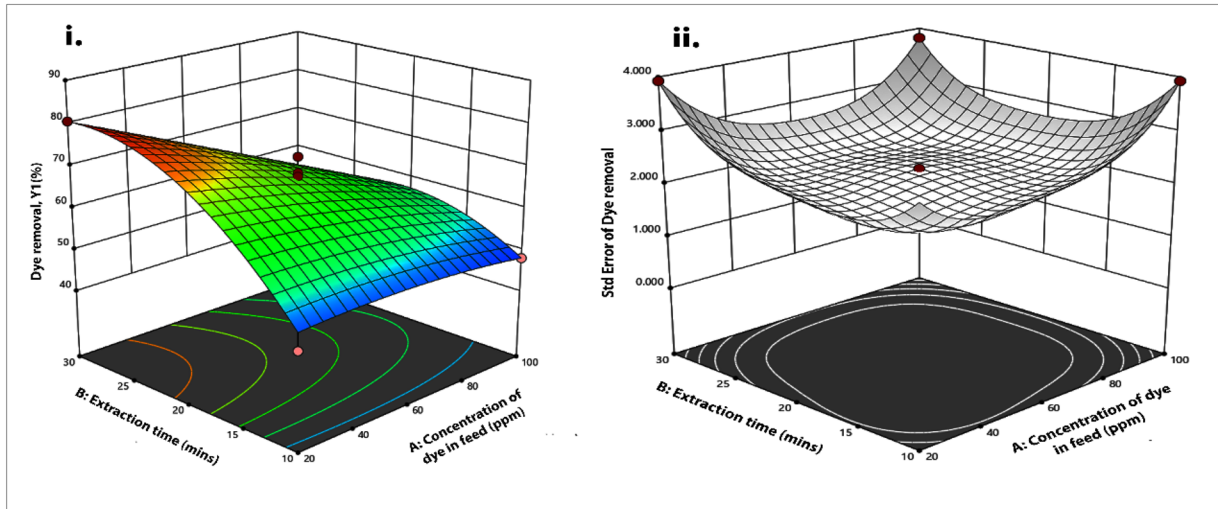
Apart from the design of the experiment (DOE), the optimization of the LLEBP parameters was accomplished using desirability function criteria. Under this technique, specific desirable values of target responses (e.g. % dye removal, distribution coefficient, and solvent capacity) were presumed, and numerical optimization was done to optimize the best process parameter values accordingly [7].

The significance of optimization depends on several factors and is linked to high-quality results. The development and stability of an optimization methodology ensures consistent reproducibility. Therefore, optimization was implemented by establishing suitable goals and checkpoints. The governing equation for the optimization process is based on the following equation:

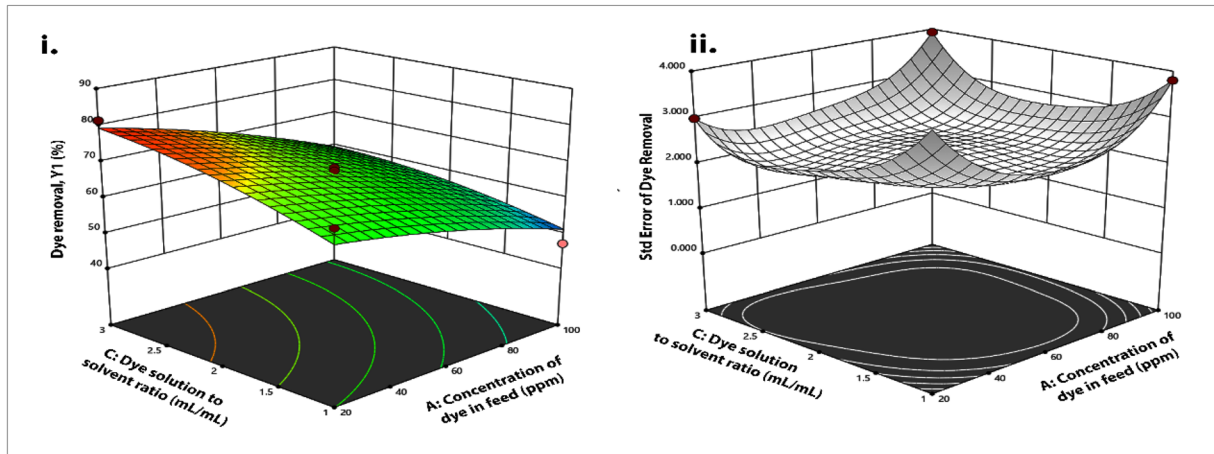
$$P(x) = \left(\prod_{i=1}^n c_i^{d_i} \right)^{1/\sum d_i} = \left(c_1^{d_1} \times c_2^{d_2} \times \dots \times c_n^{d_n} \right)^{1/\sum d_i}, \tag{7}$$

where *c_i* is the optimal range for each response, *n* denotes the number of response variables in the measurement, and P (*x*) is the desired outcome based on the weight of each response. The metric (*d_i*) spans from 1(+) to 5(++++)

a.



b.



c.

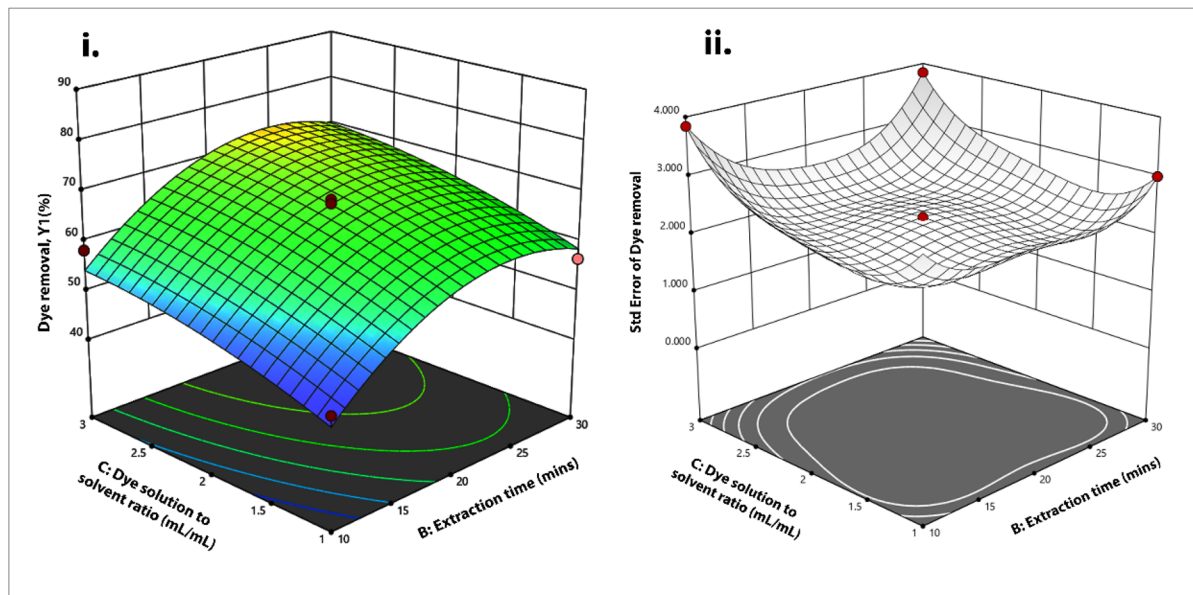


Fig. 3 The percentage of dye removed during the L–L extraction of MR dye using benzene is affected by the following factors: **a** the concentration of the dye in the feed, **b** the ratio of the dye solution to the solvent, and **c** the duration of the extraction process vs. the ratio of the dye solution to the solvent

for essential items. Normalization of an objective function occurs when all fundamental values are standardized or scaled to a common reference point. The desirability function of the response varies between 0 and 1, where undesired and desired responses are assigned values 0 and 1, respectively. These assigned values, between 0–1, indicate the degree of nearness of the response to its desired value. The ideal desirability is near 1. Hence, the desirability function helps determine the most favorable experimental factors before batch runs for achieving target goals, i.e. maximization of dye removal, optimum value of distribution coefficient and solvent capacity.

Results and Discussion

This section focuses on presenting the experimental data and interpreting the findings of this research. It involves comparing the results obtained from previously published studies to identify similarities, differences, and trends. Additionally, it aims to explain any observed discrepancies and discuss the broader implications of the findings within the context of existing literature. However, this article centres on enhancing process optimization through CCD. We're presently in the progress of sustainable industry that is in line with UN sustainable development goals like clean water and sanitation (Goal 6), decent work and economic growth (Goal 8), and industry innovation and infrastructure (Goal 9). Our research endeavors to make meaningful contributions towards addressing global challenges and advancing sustainable development.

Design of Experiments

The experimental design matrix was based on six central, eight factorial, and six axial points. The desired responses, i.e. dye removal (%), coefficient of distribution, the solvent capacity of the design matrix along with independent variables, namely initial dye concentration (ppm), dye/solvent ratio (mL/mL), and extraction time (min), are represented in terms of coded factors in second-order quadratic model equations below.

$$\begin{aligned}
 Y_1 = & 19.03 + 0.34 \times A + 5.4 \times B + 15.35 \times C \\
 & - 0.02 \times A \times B + 0.03 \times A \times C \\
 & + 0.02 \times B \times C - 9.67 \times 10^{-4} \times A^2 \\
 & - 0.09 \times B^2 - 2.00 \times C^2,
 \end{aligned} \tag{8}$$

$$\begin{aligned}
 Y_2 = & -1.18 + 0.02 \times A + 0.33 \times B + 0.94 \times C - 1.1 \times 10^{-3} \times A \times B \\
 & 2.1 \times 10^{-3} \times A \times C + 1.1 \times 10^{-3} \times B \times C - 6.0 \times 10^{-5} \times A^2 \\
 & 5.4 \times 10^{-3} \times B^2 - 0.12 \times C^2,
 \end{aligned} \tag{9}$$

$$\begin{aligned}
 Y_3 = & 0.16 + 0.64 \times A + 1.07 \times B - 10.99 \times C - 1.12 \times 10^{-3} \times A \times B \\
 & 0.122 \times A \times C - 0.13 \times B \times C - 1.3 \times 10^{-3} \times A^2 - 0.02 \times B^2 \\
 & 2.93 \times C^2.
 \end{aligned} \tag{10}$$

Coefficients A, B, and C correspond to initial dye concentration, time of extraction, and dye ratio (solution/solvent).

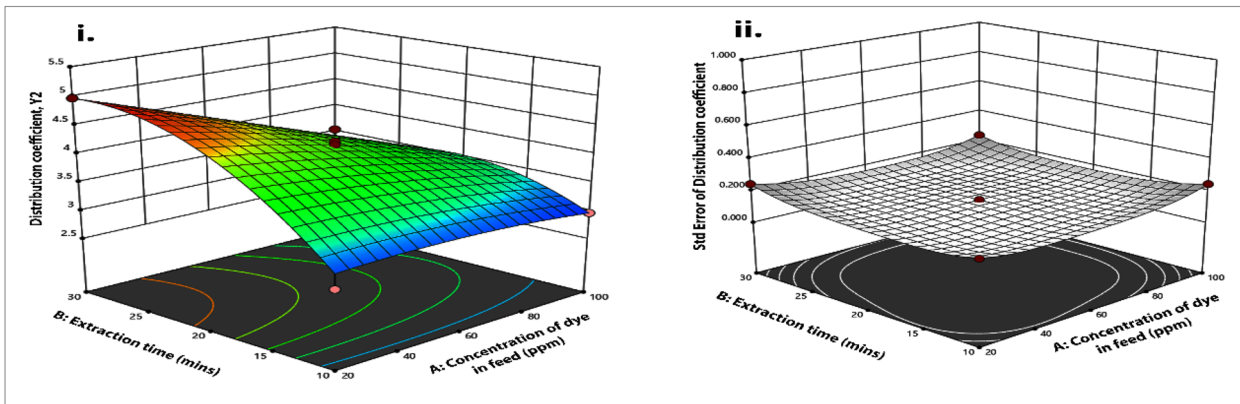
The suggested responses according to the above-mentioned mathematical models are represented in Table 2. Accordingly, batch reactions were carried out to obtain the optimum set of process parameters and the results of the responses (see Table 2 for comparison). Table 2 shows that the predicted responses from the design equation and actual batch-run data are closely matched. Hence, CCD optimization is an excellent mathematical technique for optimizing process variables with minimum inputs and achieving the best system outputs.

ANOVA Analysis of Optimized Results Related to LLEBP

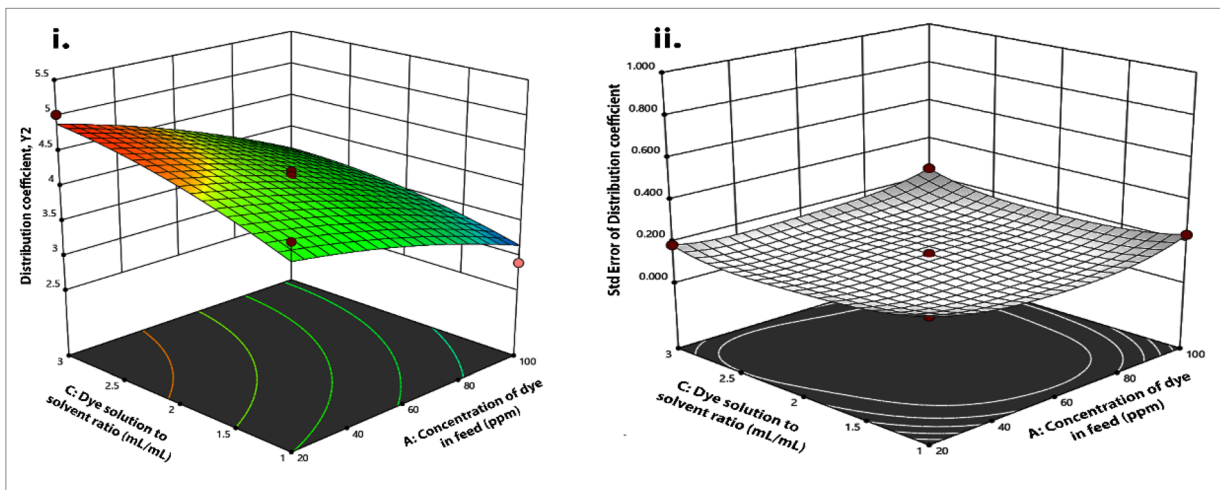
The statistical results related to the outcome of variables on LLEBP have been examined via F-test results of ANOVA analysis with a 95% confidence level. Table 3 shows the results. The assumed mathematical models are quite efficient enough for assessing the influence of process parameters on the LLEBP process with regression coefficient (R^2) values 0.9251, 0.9247, and 0.9975 for dye removal (%), coefficient of distribution, and solvent capacity. The significant effect of a specific component of the quadratic model on the desired response is evaluated with the F value (Fisher test) and P value. The threshold limit of F and P values for deciding the significant effect of a term in the model equation to modulate the dye removal % response in the current ANOVA analysis is 11.51 and 0.05, respectively (Table 3). A high F value > 11.51 and a low P value ≤ 0.05 are highly desirable.

A moderate F value (13.72) and low P value (0.0002) in the case-fitted model equation indicates the adopted model equation is manageable to optimize the % dye removal response variable. Moreover, ANOVA analysis states that not only the entire model equation, but also model coefficients (first-order terms: A, B, C; interactive terms: AB; and quadratic terms: B^2) are also substantial enough to optimize dye removal % due to the low value of P (< 0.05). Again, this could be established from the lack-of-fit term being significant (F : 242.50) and there is merely a 0.01% chance of getting it from noise. Among different optimized process parameters (Table 3), the dye concentration and

a.



b.



c.

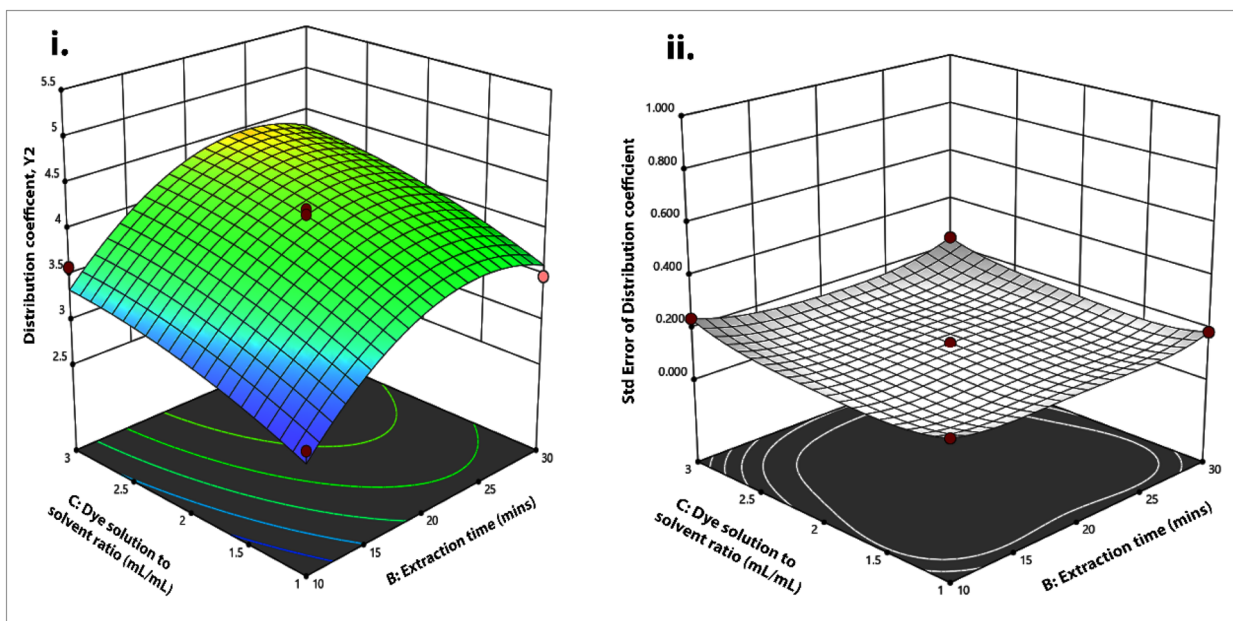


Fig. 4 The coefficient of distribution for the L–L extraction of MR dye using benzene is affected by the interactive effects of three variables: **a** the concentration of the dye in the feed vs. the duration of the extraction process, **b** the ratio of the dye solution to the solvent vs. the concentration of the dye in the feed, and **c** the duration of the extraction process vs. the ratio of the dye solution to the solvent

extraction time significantly maximize the dye removal yield due to enhanced F values of 30.73 and 28.52, respectively. The ratio of dye concentration to extractant solvent has a significantly lesser effect on dye removal % about its lesser F value (14.68). The same can be deduced for other quadratic and interactive terms such as B^2 and AB , respectively, where the comparative lower F and high P values associated with them stand against their significant contribution towards dye removal % via LLEBP.

The ANOVA analysis of the quadratic model equation employed for getting optimized solvent capacity while using the LLEBP technique for ML dye removal from wastewater is represented in Table 3. The threshold limit of F and P -magnitude for evaluating the significance of model terms to optimize the distribution coefficient (Y_2) magnitude in the current LLEBP design is 11.52 and 0.05 (see Table 3). A significantly low P – P magnitude (0.0002) in the case-fitted model equation indicates the model's suitability for optimizing the distribution coefficient value of LLEBP.

It is also observed from Table 3 that the linear terms (A , B , and C), quadratic terms (B^2), and interactive term (AB) in the model equation are substantial enough to affect the distribution coefficient value. Overall, the "dye concentration" and "extraction time" design parameters involved in the optimization process play a crucial role in optimizing the distribution coefficient value during the LLEBP experiment due to their associated high F -magnitude (> 28). Contrary to this, though the model predicts the significant role of the "dye ratio (solution/solvent)" in optimizing the distribution coefficient value, its contribution is marginal due to the lower F -magnitude (14.55). The same is the case for AB and B^2 terms.

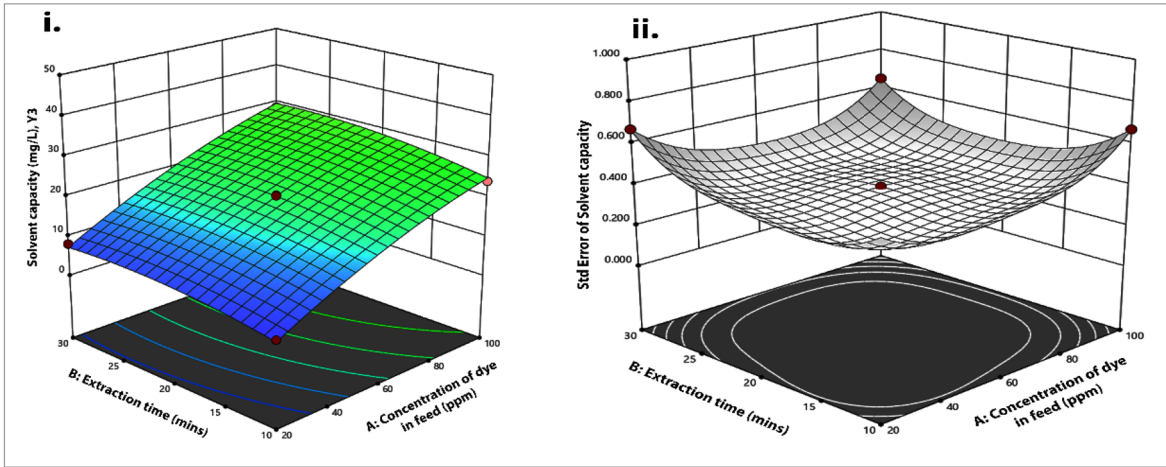
A high F -magnitude (446.73) and low P -magnitude (< 0.0001) for the fitted mathematical model shows its significance (see Table 3). However, augmented F -magnitude (75.91) and low P -magnitude (< 0.0001) observed in case of lack of fit term also suggests equally responsible linear (A , B , and C), interacting (AC , BC), and quadratic (A^2 , B^2 , and C^2) coefficients in optimizing the solvent capacity. The linear terms like dye concentration (A), as well as solvent ratio (C) and their interaction (AC), contribute significantly to the fitting of the model equation due to the high F -magnitude (> 111.84) and very low P -magnitude (< 0.0001). Though quadratic terms are considered to be significant, their contributions are marginal due to comparatively low F -magnitude.

Interactive Effect of Process Parameters on LLEBP

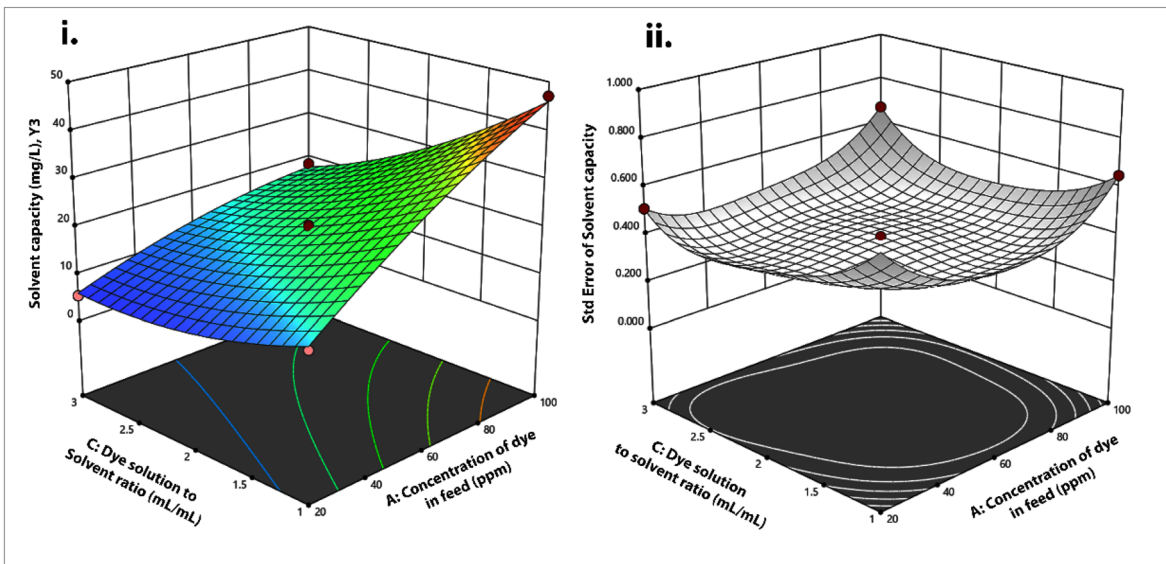
The interactive effect of the stated LLEBP parameters on dye removal (%) is studied via the optimization technique, and the corresponding 3D response plot is shown in Fig. 3. The interactive effect of both varied initial concentrations of dye in feed (20 to 100) ppm and time of extraction 10–30 min on overall dye removal (%) at a fixed dye ratio (solution/solvent) (2 mL/mL) is shown in Fig. 3a. The optimum dye removal percentage of 46.28 is achieved at the lowest dye concentration of 20 ppm and extraction time of 10 min. While increasing the content of dye in aqueous solution up to 100 ppm, the dye removal (%) improved to 48. A high dye elimination (%) is obtained (i.e. 80.57) at an optimum concentration (i.e. 20 ppm) at a specific time of extraction (i.e. 30 min). The dye removal trend decreases to 57.42% with a further increase in the dye content in the aqueous solution (up to 100 ppm) at 30 min (i.e. extraction time) and 2 mL/mL [dye ratio (solution/solvent)]. With the decrease in the extraction time (30 min to 20 min), the dye removal increases to 66.85% at 60 ppm and a predefined dye ratio (solution/solvent). From the interactive plot, it is deduced that the optimum process parameters at the fixed dye ratio (solution/solvent) (i.e. 2 mL/mL) to maximize dye removal efficacy is 20 ppm of initial dye concentration and 30 min of extraction time. The interactive effect of both varied dye concentration (20 ppm–100 ppm) and dye ratio (solution/solvent) (i.e. 1–3) mL/mL on dye elimination (%) at a fixed 20 min (i.e. extraction period) is represented in Fig. 3b. The optimum dye removal of 69.42% is achieved at low dye content (i.e. 20 ppm) and dye ratio (solution/solvent) (i.e. 1 mL/mL). With further increase in dye concentration up to 100 ppm under this condition, the dye elimination (%) decreases to 47.14. The highest dye elimination (%), 81.42, is achieved at 20 ppm and 3 mL/mL, as well as dye content and dye ratio (solution/solvent). The dye elimination (%) trend decreases to 55.71 at dye content 100 ppm and dye ratio (solution/solvent), i.e. 3 mL/mL at 20 min of extraction period.

Similarly, at a decreased dye ratio (solution/solvent) (2 mL/mL) and high value of initial dye concentration (60 ppm), the dye removal tendency is also lower (i.e. 67.71%). Hence, the optimum conditions for achieving high dye removal efficiency at a fixed extraction time of 20 min are 20 ppm of initial dye concentration and 3 mL/mL of dye ratio (solution/solvent). The interactive effect of both varied liquid–liquid extraction periods (10 to 30) min and dye ratio (solution/solvent) (1 to 3 mL/mL) on dye removal efficacy is projected in Fig. 3c. The dye concentration is fixed at 60 ppm, and at the lowest extraction time of 10 min and dye ratio (solution/solvent) of 1 mL/mL, the percentage of dye removal obtained is 45.42. With a further increasing extraction period (i.e. at 30 min), the dye removal (%) increases

a.



b.



c.

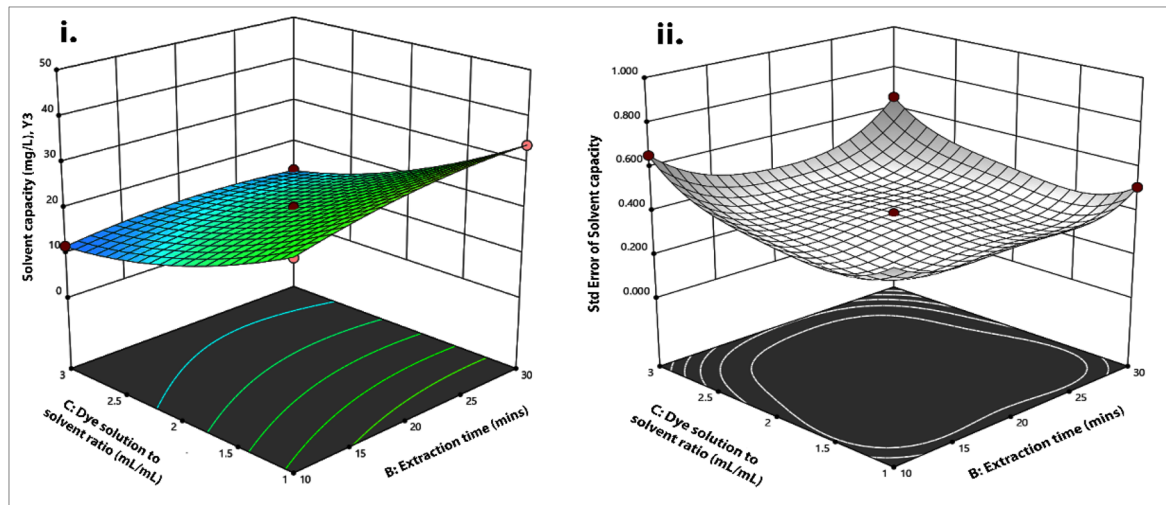


Fig. 5 The capacity of the solvent for L–L extraction of MR dye using benzene: a mutual effect of **a** the concentration of the dye in the feed vs. the duration of the extraction process and **b** the ratio of the dye solution to the solvent vs. the concentration of the dye in the feed, and **c** the duration of the extraction process vs. the ratio of the dye solution to the solvent

to 56.57. The same is the case when the dye ratio (solution/solvent) increases to 3 mL/mL, resulting in an augmented dye removal percentage of 58.28 at 10 min of extraction period. The dye removal increases to 66% with a further rise in extraction time up to 30 min at 3 mL/mL of dye ratio (solution/solvent (ratio)). A slight increase (i.e. 66.85%) in the dye removal trend is observed at a decreased dye ratio (solution/solvent) of 2 mL/mL and extraction time (i.e. 20 min). Thus, under the scenario of fixed dye concentration in the feed solution (i.e. 60 ppm), the optimum LLEBP parameters to achieve high dye removal (%) are 20 min of extraction time and 2 mL/mL of dye ratio (solution/solvent).

The interactive effect of the stated LLEBP parameters on the distribution coefficient (Y_2) is studied via the optimization technique, and the corresponding 3D response plot is shown in Fig. 4. Figure 4a shows the synergistic effect of varied dye content (20–100) ppm and extraction period (10–30) min on the Y_2 by maintaining a constant 2 mL/mL dye ratio (solution/solvent). A nominal Y_2 of 2.85 is achieved at 20 ppm (dye content) and 10 min of extraction period. At 100 ppm (dye content), the Y_2 value improved to 2.96. However, at 20 ppm dye content and a 30 min extraction period, the Y_2 enhanced to 4.97. A further decrease in the Y_2 value of 3.54 was observed upon increasing the dye content (i.e. 100 ppm) and extraction period of 30 min. Even on lowering the extraction time (20 min) and dye concentration (60 ppm) value, the maximum Y_2 obtained is 4.17. Hence, from the 3D response plot, it can be postulated that to achieve maximum distribution coefficient at a fixed dye ratio (solution/solvent) (2 mL/mL), the optimum process parameters under the current experimental scenario are 20 ppm of dye concentration and 30 min of extraction time.

Similarly, the interactive effect of dye content in aqueous solution and dye ratio (solution/solvent) on the Y_2 at a constant 20 min (extraction period) is represented in Fig. 4b. A high $Y_2 = 4.28$ is achieved at the lowest dye content (20 ppm) and dye ratio (solution/solvent) of 1 mL/mL. Upon increasing the dye concentration to 100 ppm at 1 mL/mL of dye ratio (solution/solvent), the Y_2 value decreased to 2.90. Maximum $Y_2 = 5.02$ was obtained at an optimum dye content of 20 ppm and dye ratio (solution/solvent) of 3 mL/mL. Y_2 remains low at 3.43 at 100 ppm (dye content) and 3 mL/mL of dye ratio (solution/solvent) by keeping the extraction time constant (i.e. 20 min). Even after decreasing the dye ratio (solution/solvent) to 2 mL/mL and dye content

of 60 ppm, the Y_2 value did not much improve beyond 4.23. Hence, under the current scenario, the optimal conditions are proposed to be 20 ppm of dye concentration and 3 mL/mL of dye ratio (solution/solvent) to achieve maximum Y_2 . The interaction between the dye ratio (solution/solvent) and extraction time is examined via the RSM technique, and the corresponding response plot for the Y_2 is shown in Fig. 4c. Maintaining a fixed dye content (i.e. 60 ppm) at 10 min extraction time and 1 mL/mL dye ratio (solution/solvent), the Y_2 value obtained is 2.8.

Further increasing the extraction time at this condition to 30 min, the Y_2 value improved to 3.49. Similarly, keeping the extraction time fixed at 10 min and increasing the dye ratio (solution/solvent) to 3 mL/mL Y_2 enhanced it to 3.59. This value can be further improvised to 4.07 by increasing the extraction time to 30 min. Further improvement in the Y_2 value (4.17) is accomplished by reducing the dye ratio (solution/solvent) to 2 mL/mL and the extraction time to 20 min. Hence, from the 3D response plot, it can be deduced that the optimum time and dye solution/solvent ratio under such conditions are 20 min and 2 mL/mL, respectively, to obtain the maximum Y_2 . The interactive effect of the stated LLEBP parameters on solvent capacity is studied via optimization technique, and the corresponding 3D response plot is shown in Fig. 5. Figure 5a shows the synergistic response in terms of a 3D plot regarding variation in the dye content and extraction period on the solvent capacity value while maintaining a constant dye ratio (solution/solvent) (2 mL/mL). When the dye content in the feed solution is 20 ppm and the extraction period applied is 10 min, a low solvent capacity value is obtained as 4.62 mg/L. At a maximum dye concentration value of 100 ppm, under 10 min of extraction time, an augmented solvent capacity value of 24 mg/L is obtained. However, when the feed concentration decreased to 20 ppm and the extraction period enhanced to 30 min, the solvent capacity was lowered to 8.05 mg/L.

On the contrary, the solvent capacity can be improved to 28.71 mg/L at a high feed concentration of 100 ppm by maintaining the extraction period at 30 min. The solvent capacity value still improved to 20.05 mg/L by decreasing the extraction period to 20 min, but at the expense of higher dye content (i.e. 60 ppm). Hence, from the response plot Fig. 5a, it can be postulated that an optimum dye concentration of 100 ppm in feed and at 30 min extraction time, the maximum solvent capacity value can be obtained. Figure 5b shows the interactive effect of varied dye content and dye ratio (solution/solvent) on optimizing the solvent capacity at a fixed extraction time of 20 min. The solvent capacity value of 13.88 mg/L is obtained at 20 ppm of feed concentration and 1 mL/mL of dye ratio (solution/solvent). At the highest dye concentration value, 100 ppm, a solvent capacity value obtained is 47.14 mg/L while keeping the dye ratio

Table 4 Numerical optimization of process parameters as desirability function criteria

No	Dye conc. (ppm)	Extraction time (min)	Dye solution/solvent (ratio)	% Dye Removal	Distribution coefficient	Solvent capacity (mg/L)	Desirability
1	20.000	30.000	3.000	85.682	5.287	4.504	0.992 (selected)
2	20.000	29.998	3.000	85.683	5.287	4.504	0.992
3	20.000	29.905	2.999	85.704	5.288	4.534	0.992
4	20.000	29.787	3.000	85.733	5.290	4.571	0.992

(solution/solvent) at 1 mL/mL. A deficient solvent capacity (5.42 mg/L) is achieved at the feed concentration of 20 ppm and dye ratio (solution/solvent) of 3 mL/mL.

Further improvement in the solvent capacity value (18.57 mg/L) is accomplished when the feed concentration is increased to 100 ppm at 3 mL/mL of dye ratio (solution/solvent). By decreasing the value of the dye ratio (solution/solvent) (2 mL/mL) and feed dye concentration (60 ppm), the solvent capacity can still improve to 20.57 mg/L, but not beyond that. Hence, the optimal conditions for achieving maximum solvent capacity under the current experimental scenario are 100 ppm of dye concentration and 1 mL/mL dye ratio (solution/solvent). Figure 5c shows the 3D response plot of solvent capacity examined under varied conditions of extraction time (10–30) min and dye ratio (solution/solvent) (1 to 3) mL/mL by keeping the feed concentration constant at 60 ppm. The solvent capacity value of 27.25 mg/L is observed at 10 min (extraction period), and the dye ratio (solution/solvent) is 1 mL/mL. If extraction time increased to 30 min at the predefined dye ratio (solution/solvent), the solvent capacity improved to 33.94 mg/L. However, the solvent capacity decreased to 11.65 mg/L by reducing the extraction time (10 min) and increasing the dye ratio (solution/solvent) (3 mL/mL). This value can still improve to 13.2 mg/L by increasing the extraction time (30 min) at a dye ratio (solution/solvent) of 3 mL/mL. Further improvement in the solvent capacity can be achieved (20.57 mg/L) by decreasing the dye ratio (solution/solvent) to 2 mL/mL and 20 min (extraction period). Thus, under the defined dye concentration constraint (60 ppm) to achieve maximum solvent capacity, optimal process conditions would be 30 min of extraction period and 1 mL/mL of dye ratio (solution/solvent). Other researchers have observed similar results [18].

Overall, from the design of the experiments, it can be postulated that to carry out the batch method of LLEBP for dye removal under specified process conditions, the optimum process variables required can range from (20 to 30) ppm for dye content, (20 to 30) min for extraction period, and (1 to 3) mL/mL for dye ratio (solution/solvent) to maximize dye removal (%) and Y_2 value. However, these optimized process parameters are unsuitable enough to maximize the solvent capacity under the current adopted LLEBP

experiments. Moreover, the maximum solvent capacity value can be achieved by increasing the feed concentration range from (60 to 100) ppm by keeping all other selected process ranges described before. Moreover, the previously reported BBD optimization technique by Kanakasabai et al. (2023) [34] demonstrated less removal (%). On the other hand, CCD techniques employed by some other researchers [45, 47] achieved better results for similar studies. This study has been carried out within the same input range as previous MR dye removal studies. Figure 3a.ii, b.ii, c.ii shows the dye removal (%); Fig. 4a.ii, b.ii, c.ii depicts the coefficient of distribution; and Fig. 5a.ii, b.ii and c.ii shows the capacity of the solvent; at a specific coordinate in the factor space, it shows the standard error. The outcomes vary from 1 → 4 for the percentage of dye removed, 0.1 → 0.3 for the coefficient of distribution, and 0.35 → 0.7 for the capacity of the solvent.

Ascertaining Optimum LLEBP Process Conditions by Desirability Function Criteria

The numerical optimization using the Design Expert 13 is examined towards various factors of the LLEBP experiment and corresponding responses to ascertain suitable batch reaction conditions. From the available criteria embedded in the software (range selection, maximization/minimization, target), achieving maximum value for all the previously stated response variables is accomplished via numerical optimization techniques focusing on the desirability criteria. Since many batch runs are required in the optimization process, they can consume much time and energy. RSM-CCD design and the numerical optimization based on the desirability function are applied for all three stated LLEBP [7, 16]. The target response for dye removal yield, distribution coefficient, and solvent capacity is 85–90%, 5–6, and 4–5 mg/mL, respectively. Though the value of solvent capacity is very much high, as anticipated in the DOE technique, this value is optimum under the current context of the selected process parameter range. The default importance setting (+ + + +) is allotted to all the LLEBP process variables, significantly affecting the response variables. Equal weight (1) is allocated to all the

Fig. 6 a Part 1: optimizing the LLEBP process parameters (dye conc. and extraction time) to get maximum process yield using the desirability criteria, Part 2: contour plot showing the effect on % dye removal, Part 3: effect on the distribution coefficient, Part 4: effect on solvent capacity. **b** Part 1: optimizing the LLEBP process parameters [dye conc. and dye ratio (solution/solvent)] is used to get the maximum process yield using the desirability criteria. Part 2: contour plot showing the effect on % dye removal. Part 3: effect on the distribution coefficient. Part 4: effect on solvent capacity. **c** Part 1: optimizing the LLEBP process parameters [extraction time and dye ratio (solution/solvent)] for getting maximum process yield using the desirability criteria. Part 2: contour plot showing the effect on % dye removal. Part 3: effect on distribution coefficient. Part 4: effect on solvent capacity

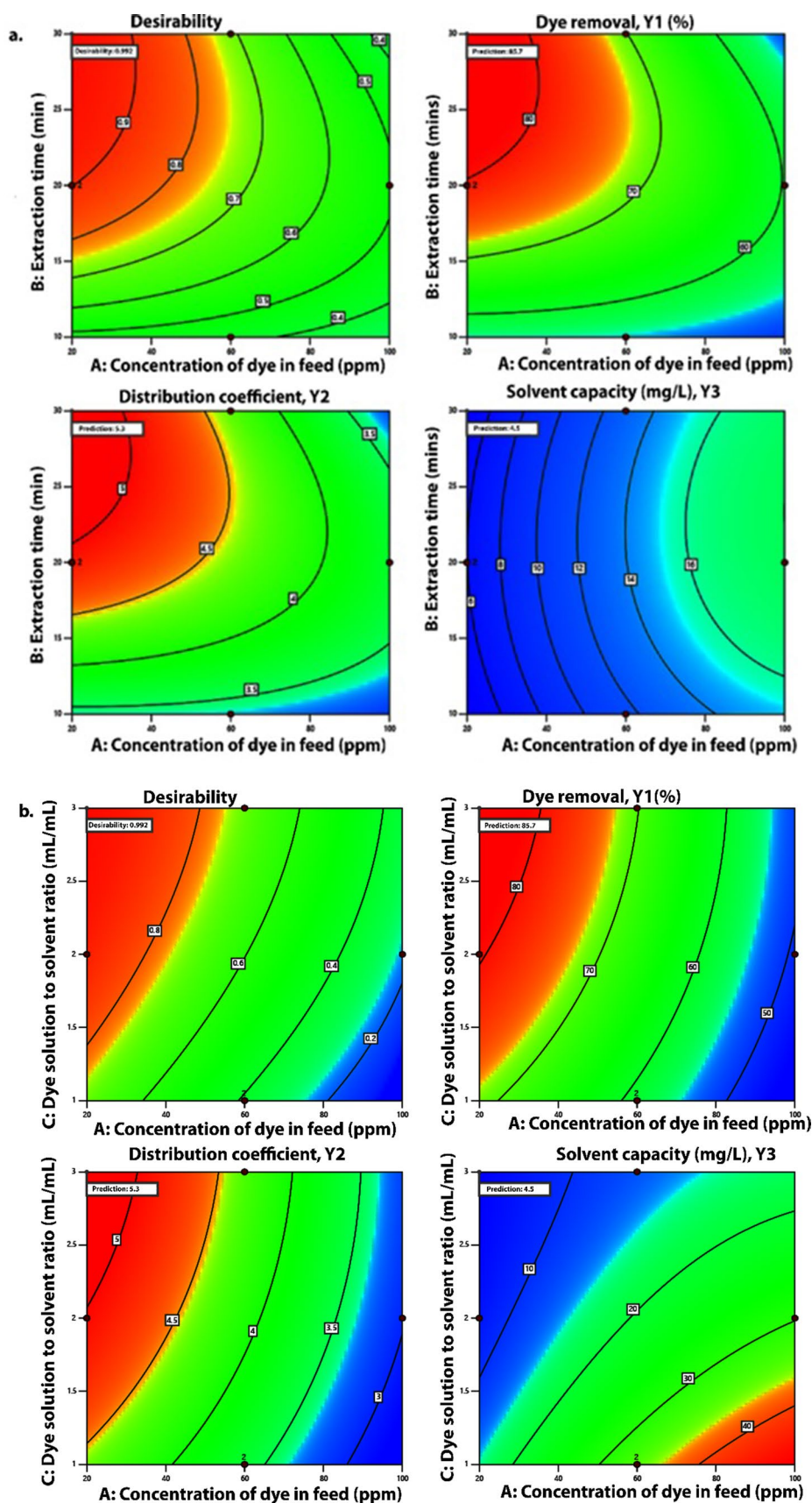
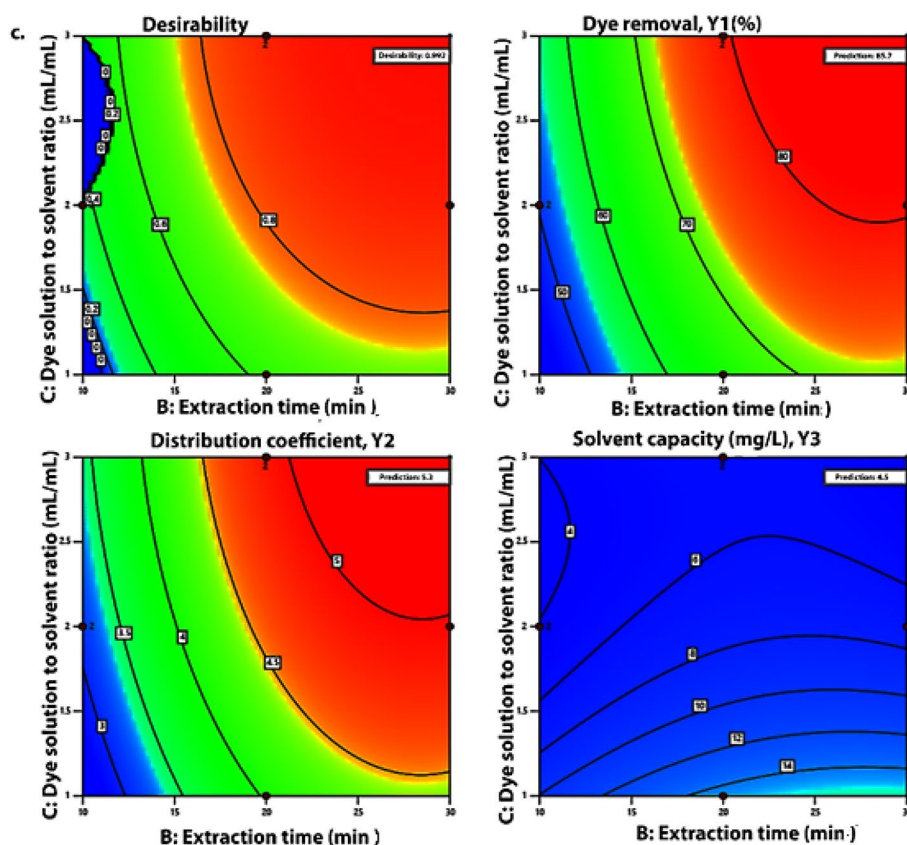


Fig. 6 (continued)



dependent and independent factors. Table 4 displays the optimization outcomes for dye removal (%) and distribution coefficient values obtained from LLEBP experiments. These results were derived from batch runs conducted at an initial dye concentration of 20 ppm, an extraction time of 30 min, and a dye ratio of 3 mL/mL (solution/solvent). The subsequent result of the numerical optimization is depicted in Table 4, and the corresponding contour plots are shown in Figs. 6 (see Figs. 6a, b, c).

From Table 4., it can be ascertained that by taking into account the desirability function criteria, numerical optimization via design expert is very helpful in minimizing the variation in the process parameters. The optimization of dye removal (%) and distribution coefficient values in LLEBP experimental conditions is provided in Table 4. These conditions fall within the range of process parameters earlier predicted by the design of the technique of the experiment. Hence, the optimization process can be more precise, excluding unwanted and time-consuming batch runs. Regarding the desirability of "solvent capacity" falling within the ascertained range of process variables, the numerical optimization technique also adopted accurate estimates. However, the actual results can be achieved at higher feed concentration ranges. The corresponding contour plots related to optimized responses are provided in Fig. 6 based

on a 0.992 (~ 1) desirability factor. The red and blue colours represent desirable values of 1 (high) and 0 (low). The desirable values for % dye removal and distribution coefficient align with the selected process parameters range and show good optimization fit (red colour). However, the chosen desirable value for solvent capacity doesn't fall well with the optimized process variables range; thus, intense blue is observed in the contour plots. Indeed, optimization via desirability function criteria is an excellent way of ascertaining narrow and specific process variable ranges without going for labour some unwanted batch reactions.

Flow Sheet of the Dye Removal Process

A flow sheet proposed to remove and recover methyl red dye from industrial wastewater is shown in Fig. 7.

The prepared model oil or wastewater containing dye is mixed with benzene, allowing the dye to dissolve in the benzene. The aqueous solution is then separated from the organic solvent. The organic solvent is subsequently mixed with NaOH, and another phase separation is performed. The aqueous phase is analysed to determine if the desired limits are achieved. If the desired limits are not met, the process is repeated until they are. The separated organic phase is then reused.

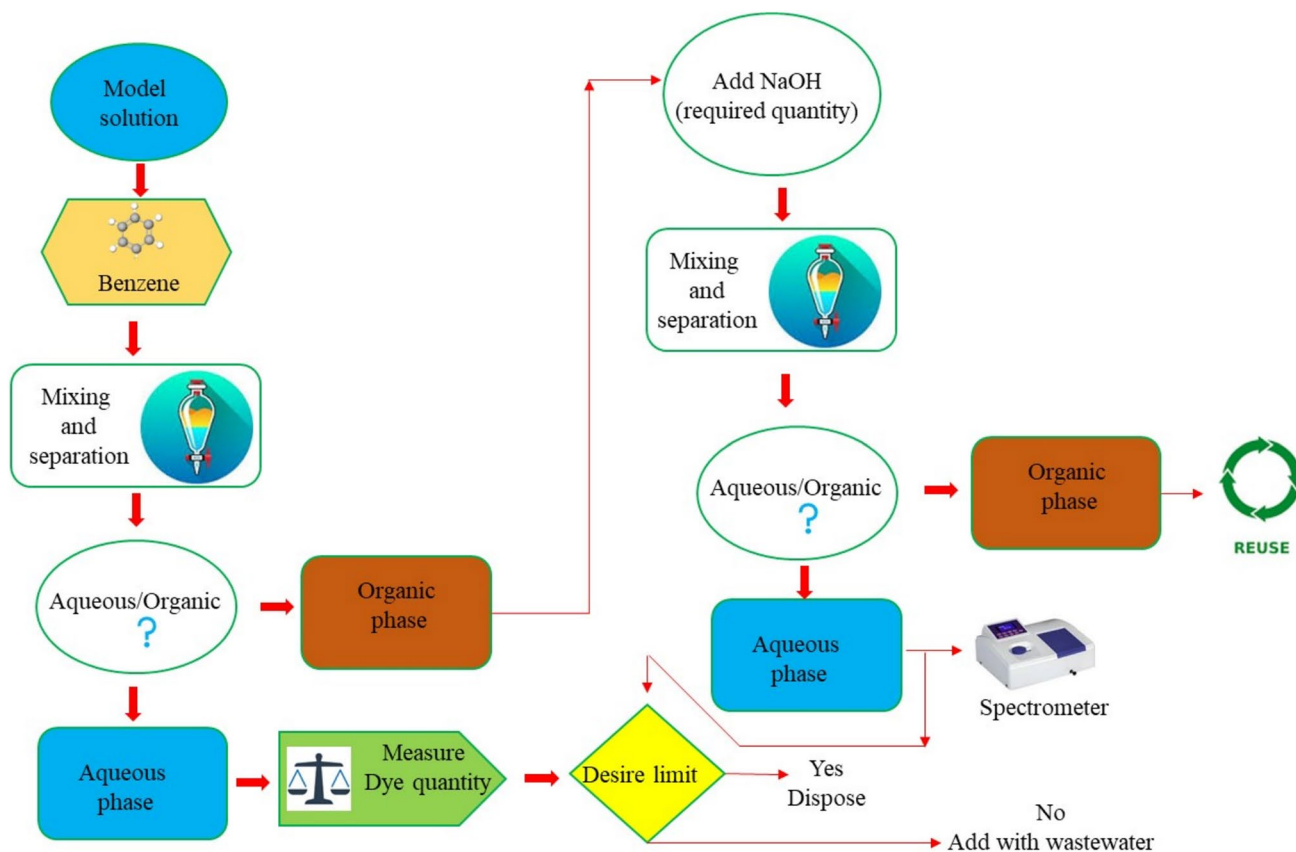


Fig. 7 Proposed flow diagram for extraction and recovery of the red dye from wastewater

Conclusion

The current study demonstrates the effective use of numerical optimization techniques to determine the optimal range of LLEBP process parameters for the efficient removal of MR dye from model textile dye effluent, avoiding the laborious OVAT method. Key process variables such as dye concentration in the feed, extraction time, and dye ratio (solution/solvent) were optimized to achieve high dye removal yield, solvent capacity, and distribution coefficient at a constant pH of 3 and room temperature.

The design of the experiments using quadratic model equations indicated that an optimal range for the selected variables—dye concentration: (20–30) ppm, extraction time: (20–30) min, and dye ratio (solution/solvent): (1–3) mL/mL—resulted in dye removal percentages as high as 80–85%. Similar conditions yielded a high LLEBP distribution coefficient (~5 to 5.5 mg/L) and solvent capacity (~40 to 50 mg/L), with slight modifications to the design range. The desirability function criteria further refined these variables, identifying optimal conditions: 20 ppm dye concentration, 30 min extraction time, and a 3 mL/mL dye ratio.

These conditions achieved a dye removal yield of 85.682%, a distribution coefficient of 5.287, and a solvent capacity of 4.504 mg/L.

Although the selected variables did not achieve the highest possible solvent capacity, the obtained value was higher compared to other studies using BBD. This research effectively designs experimental variables for maximum LLEBP efficacy in MR dye removal using the CCD optimization technique instead of BBD with the same input data. The response surface diagrams demonstrated exceptional goodness-of-fit between the experimental and predicted values.

Additionally, our results enhance the understanding of optimizing the extraction process for improved dye removal from model textile effluent, contributing to environmental sustainability. This study aims to maximize process optimization using CCD, aligning with UN sustainability goals, and offers significant contributions to the fields of environmental remediation and wastewater treatment. The findings provide valuable insights for developing efficient and sustainable industrial wastewater treatment systems.

Acknowledgements This work was supported by the National Research Foundation of Korea (NRF) grant funded by the Korea government (MSIT) (No. 2021R1A2C2006888).

Authors' Contributions Kedar Sahoo: conceptualization, methodology, writing—original draft, validation; Uma Sankar Behera: conceptualization, methodology, writing—original draft, visualization, validation; Sourav Poddar: conceptualization, methodology, writing original draft, visualization, validation; Hun-Soo Byun: supervision, review and editing, funding acquisition, visualization, validation, project administration.

Data availability All relevant data supporting the findings of this study are included within the article.

Declarations

Conflict of Interest There are no conflicts of interest to disclose.

References

1. K. Shradha, J. Dipika, M. Arti, Green and Eco-Friendly Materials for the Removal of Phosphorus from Wastewater, in *Life Cycle Assess Wastewater Treat.* ed. by M. Naushad, M. Naushad (CRC Press, Boca Raton, 2018), pp.199–211
2. J.K. Adusei, E.S. Agorku, R.B. Voegborlo, F.K. Ampong, B.Y. Danu, F.A. Amarh, *Sci. Afr.* **17**, e01273 (2022)
3. R. Ahmad, R. Kumar, *Appl. Surf. Sci.* **257**, 1628 (2010)
4. R. Ahmad, R. Kumar, *J. Environ. Manage.* **91**, 1032 (2010)
5. M. Shafiqul Alam, *J. Environ. Prot.* **4**, 207 (2015)
6. A.R. Omran, M.A. Baiee, S.A. Juda, J.M. Salman, A.F. AlKaim, *Int. J. Chem. Tech. Res.* **9**, 334 (2016)
7. U.S. Behera, S. Poddar, H.S. Byun, *J. Chem. Technol. Biotechnol.* **99**, 1212 (2024)
8. N.Y. Donkadokula, A.K. Kola, I. Naz, D. Saroj, *Rev. Environ. Sci. Biotechnol.* **19**, 543 (2020)
9. S. Gul, M. Kanwal, R.A. Qazi, H. Gul, R. Khattak, M.S. Khan, F. Khitab, A.E. Krauklis, *Water* **14**, 2831 (2022)
10. E. Fosso-Kankeu, A. Webster, I.O. Ntwampe, F.B. Waanders, *Arab. J. Sci. Eng.* **42**, 1397 (2017)
11. S.S. Ashraf, M.A. Rauf, S. Alhadrami, *Dye. Pigment.* **69**, 74 (2006)
12. M. Zhou, Q. Yu, L. Lei, G. Barton, *Sep. Purif. Technol.* **57**, 380 (2007)
13. X.H. Cheng, W. Guo, *Dye. Pigment.* **72**, 372 (2007)
14. E.E. Rios-Del Toro, L.B. Celis, F.J. Cervantes, J.R. Rangel-Mendez, *J. Hazard. Mater.* **260**, 967 (2013)
15. P. Sarkar, A. Fakhruddin, M.K. Pramanik, *Int. J. Environ.* **1**, 34 (2011)
16. M. Ikram, M. Naeem, M. Zahoor et al., *Int. J. Environ. Res. Public Health* **19**, 9962 (2022)
17. N. Sharifi, A. Nasiri, S. Silva Martínez, H. Amiri, *J. Photochem. Photobiol. A Chem.* **427**, 113845 (2022)
18. M.V. Ratnam, C. Karthikeyan, K.N. Rao, V. Meena, *Mater. Today Proc.* **26**, 2308 (2019)
19. A. Bes-Piña, J.A. Mendoza-Roca, M.I. Alcaina-Miranda, A. Iborra-Clar, M.I. Iborra-Clar, *Desalination* **157**, 73 (2003)
20. D. Georgiou, A. Aivazidis, J. Hatiras, K. Gimouhopoulos, *Water Res.* **37**, 2248 (2003)
21. A. Baban, A. Yediler, D. Lienert, N. Kemerdere, A. Kettrup, *Dye. Pigment.* **58**, 93 (2003)
22. T. Kurbus, Y.M. Slokar, A.M. Le Marechal, D.B. Vončina, *Dye. Pigment.* **58**, 171 (2003)
23. P. Jain, K. Sahoo, L. Mahiya, H. Ojha, H. Trivedi, A.S. Parmar, M. Kumar, *J. Environ. Manage.* **281**, 11797 (2021)
24. S. Moosavi, C.W. Lai, S. Gan, G. Zamiri, O.A. Pivezhani, M.R. Johan, *ACS Omega* **5**, 20684 (2020)
25. G. Muthuraman, T.T. Teng, *Prog. Nat. Sci.* **19**, 1215 (2009)
26. W. Shi, L. Wang, D.P.L. Rousseau, P.N.L. Lens, *Environ. Sci. Pollut. Res.* **17**, 824 (2010)
27. P. Pandit, S. Basu, *J. Colloid Interface Sci.* **245**, 208 (2002)
28. H. Hu, M. Yang, J. Dang, *Sep. Purif. Technol.* **42**, 129 (2005)
29. A. Yilmaz, E. Yilmaz, M. Yilmaz, R.A. Bartsch, *Dye. Pigment.* **74**, 54 (2007)
30. M. Regel-Rosocka, J. Szymanowski, *Chemosphere* **60**, 1151 (2005)
31. G. Muthuraman, T.T. Teng, C.P. Leh, I. Norli, *J. Hazard. Mater.* **163**, 363 (2009)
32. G. Muthuraman, K. Palanivelu, *Indian J. Chem. Technol.* **11**, 166 (2004)
33. A. Abbasi, Z. Seifollahi, A. Rahbar-Kelishami, *Sep. Sci. Technol.* **56**, 1047 (2021)
34. P. Kanakasabai, S. Sivamani, K. Thirumavalavan, *Chem. Pap.* **77**, 7225 (2023)
35. M.A. Bezerra, R.E. Santelli, E.P. Oliveira, L.S. Villar, L.A. Escaleira, L. Silveira Villar, L.A. Elia Escaleira, *Talanta* **76**, 965 (2008)
36. L. Ye, M. Yang, L. Xu, C. Guo, L. Li, D. Wang, *J. Meas. Int. Meas. Confed.* **48**, 252 (2014)
37. M. Amidi, E. Salehi, *Korean J. Chem. Eng.* **40**, 2384 (2023)
38. M. Ranga, S. Sinha, P. Biswas, *Korean J. Chem. Eng.* **40**, 2219 (2023)
39. M. Noormohammadi, M. Zabihi, M. Faghihi, *Korean J. Chem. Eng.* **41**, 1535 (2024)
40. U.S. Behera, P.C. Mishra, G.B. Radhika, *Water Sci. Technol.* **85**, 515 (2022)
41. D.C. Montgomery, *Design and Analysis of Experiments, 10th Edition* (Wiley, New York, 2019)
42. M.B. Kasiri, H. Aleboyeh, A. Aleboyeh, *Environ. Sci. Technol.* **42**, 7970 (2008)
43. S. Poddar, *Int. J. Innov. Technol. Explor. Eng.* **9**, 1428 (2020)
44. S. Poddar, J.S.C. Babu, *Renew. Energy* **175**, 253 (2021)
45. S. Poddar, J. Khanam, *J. Mol. Liq.* **351**, 11862701 (2022)
46. S. Karmakar, S. Poddar, J. Khanam, *AAPS PharmSci. Tech.* **23**, 25601 (2022)
47. S. Poddar, J. Khanam, P. Pradhan, *J. Chem. Technol. Biotechnol.* **98**, 898 (2023)
48. A. El-Ghenymy, S. Garcia-Segura, R.M. Rodríguez, E. Brillas, M.S. Begrani, B.A. Abdelouahid, *J. Hazard. Mater.* **221**, 288 (2012)
49. D. Baskaran, P. Saravanan, V. Saravanan, R.R. Kannan, S. Ramesh, M. Dilipkumar, R. Muthuvelayudham, *Biomass Convers. Biorefin.* **14**, 6435 (2024)

Publisher's Note Springer Nature remains neutral with regard to jurisdictional claims in published maps and institutional affiliations.

Springer Nature or its licensor (e.g. a society or other partner) holds exclusive rights to this article under a publishing agreement with the author(s) or other rightsholder(s); author self-archiving of the accepted manuscript version of this article is solely governed by the terms of such publishing agreement and applicable law.